Shape Evolution of ZnTe Nanocrystals: Nanoflowers, Nanodots, and Nanorods

Sang Hyun Lee, Yun Ju Kim, and Jeunghee Park*

Department of Chemistry, Korea University, Jochiwon 339-700, Korea

Received April 27, 2007. Revised Manuscript Received July 6, 2007

We synthesized highly crystalline zinc telluride (ZnTe) nanocrystals with a controlled shape using various growth conditions. The following amines were used as activation agents for the zinc precursor: zinc stearate, octylamine (OA), dodecylamine (DDA), octadecylamine (ODA), and trioctylamine (TOA). Unique 3-D nanoflowers (av size = 20−120 nm) that consisted of a number of nanodots (av size = 4−11 nm) were efficiently produced when no amine or TOA was used. Dispersed nanodots were produced when OA, DDA, or ODA were used. These results indicate that the steric effect of alkyl chains plays an important role in the formation of nanoflowers. Furthermore, the shape evolution from nanoflowers to nanorods occurred at higher growth temperatures, and nanoflowers and nanorods eventually evolved into nanodots after incubation.

Introduction

Colloidal II−VI semiconductor nanocrystals (NCs) are of great interest for fundamental studies (i.e., quantum size effects) and because of their promising applications in the field of light-emitting diodes (LEDs),[1] lasers,[2] solar cells,[3] gas sensors,[4] and biomedical labeling.[5] NCs exhibit unique optical and electronic properties depending on their size and shape, which are distinct from those of the corresponding bulk counterparts.[6−8] Therefore, control of the size and shape of NCs has been the most important issue in the synthesis of NCs and has advanced dramatically in the past few years.[9−11] Zinc telluride (ZnTe), which has a direct gap of 2.26 eV (ca. 548 nm) at room temperature, is an attractive semiconductor material for various optoelectronic devices, such as green LEDs and solar cells.[12,13] However, size- and shape-controlled synthesis of colloidal ZnTe NCs has received little attention as compared to that of other chalcogenides (e.g., CdSe). The synthesis of spherical and rod-like NCs was demonstrated using a single molecular precursor ([$Zn(TePh)_2$][TMEDA]) by Cheon and co-workers.[14] Recently, the synthesis of ZnTe/CdSe (or CdS, CdTe) core/shell spherical NCs with varied core sizes and shell thicknesses, as well as their widely tuned emission from the visible to near-infrared regions, was reported by Basché and co-workers.[15] Conversely, ZnTe nanorods were preferentially synthesized using autoclave reactions.[16,17]

Here, we report the synthesis of high-quality ZnTe NCs with their size and shape controlled by changing the ligands and the growth temperature and time. Trioctylphosphine (TOP) or tributylphosphine (TBP) was used as the activating agent for Te, forming a TOP−Te (or TBP−Te) complex, in the non-coordinating solvent, 1-octadecene (ODE). The concentration of TOP and TBP was adjusted to control the size and shape of the ZnTe NCs. The following amines were used as activation agents for the zinc precursor: zinc stearate ($Zn(St)_2$), octylamine (OA), dodecylamine (DDA), octadecylamine (ODA), and trioctylamine (TOA). Specifically, the amines, strong electron-donating ligands, were used to attack the carbonyl group of $Zn(St)_2$, resulting in oxide intermediates being formed that were then easily attacked by Te.[18] They can also act as sufficient protection or limited protection ligands, determining the shape of the nanocrystals, as will be discussed later.[19] Moreover, the shape evolution from aggregated nanodots to dispersed nanodots as well as to nanorods was achieved by altering the growth temperature and time.

* Corresponding author. E-mail: parkjh@korea.ac.kr.

(1) Tessler, N.; Medvedev, V.; Kazes, M.; Kan, S.; Banin, U. *Science* **2002**, *295*, 1506.
(2) Wang, C.; Wehrenberg, B. L.; Woo, C. Y.; Guyot-Sionnest, P. *J. Phys. Chem. B* **2004**, *108*, 9027.
(3) Gur, I.; Fromer, N. A.; Geier, M. L.; Alivisatos, A. P. *Science* **2005**, *310*, 462.
(4) Nazzal, A. Y.; Qu, L.; Peng, X.; Xiao, M. *Nano Lett.* **2003**, *3*, 819.
(5) Mulder, W. J. M.; Koole, R.; Brandwijk, R. J.; Storm, G.; Chin, P. T. K.; Strijkers, G. J.; de Mello Donegá, C.; Nicolay, K.; Griffioen, A. W. *Nano Lett.* **2006**, *6*, 1.
(6) Kagan, C. R.; Murray, C. B.; Bawendi, M. G. *Phys. Rev. B* **1996**, *54*, 8633.
(7) Peng, X.; Manna, U.; Yang, W.; Wickham, J.; Scher, E.; Kadavanich, A.; Alivisatos, A. P. *Nature* **2000**, *404*, 59.
(8) Chen, X.; Nazzal, A.; Goorskey, D.; Xiao, M.; Peng, Z. A.; Peng, X. *Phys. Rev. B* **2001**, *64*, 245304.
(9) Peng, Z. A.; Peng, X. *J. Am. Chem. Soc.* **2002**, *124*, 3343.
(10) Manna, L.; Scher, E. C.; Alivisatos, A. P. *J. Am. Chem. Soc.* **2000**, *122*, 12700.
(11) Pradhan, N.; Xu, H.; Peng, X. *Nano Lett.* **2006**, *6*, 720.
(12) Crowder, B. L.; Morehead, F. F.; Wagner, P. R. *Appl. Phys. Lett.* **1966**, *8*, 148.
(13) Bhunia, S.; Bose, D. N. *J. Cryst. Growth* **1998**, *186*, 535.
(14) Jun, Y.; Choi, C.-S.; Cheon, J. *Chem. Commun.* **2001**, 101.
(15) Xie, R.; Zhong, X.; Basché, T. *Adv. Mater.* **2005**, *17*, 2741.
(16) Li, Y.; Ding, Y.; Wang, Z. *Adv. Mater.* **1999**, *11*, 847.
(17) Du, J.; Xu, L.; Zou, G.; Chai, L.; Qian, Y. *J. Cryst. Growth* **2006**, *291*, 183.
(18) Li, L. S.; Pradhan, N.; Wang, Y.; Peng, X. *Nano Lett.* **2004**, *4*, 2261.
(19) (a) Narayanaswamy, A.; Xu, H.; Pradhan, N.; Peng, X. *Angew. Chem., Int. Ed.* **2006**, *45*, 5361. (b) Narayanaswamy, A.; Xu, H.; Pradhan, N.; Kim, M.; Peng, X. *J. Am. Chem. Soc.* **2006**, *128*, 10310.

10.1021/cm0711360 CCC: $37.00
Published on Web 08/18/2007

Scheme 1

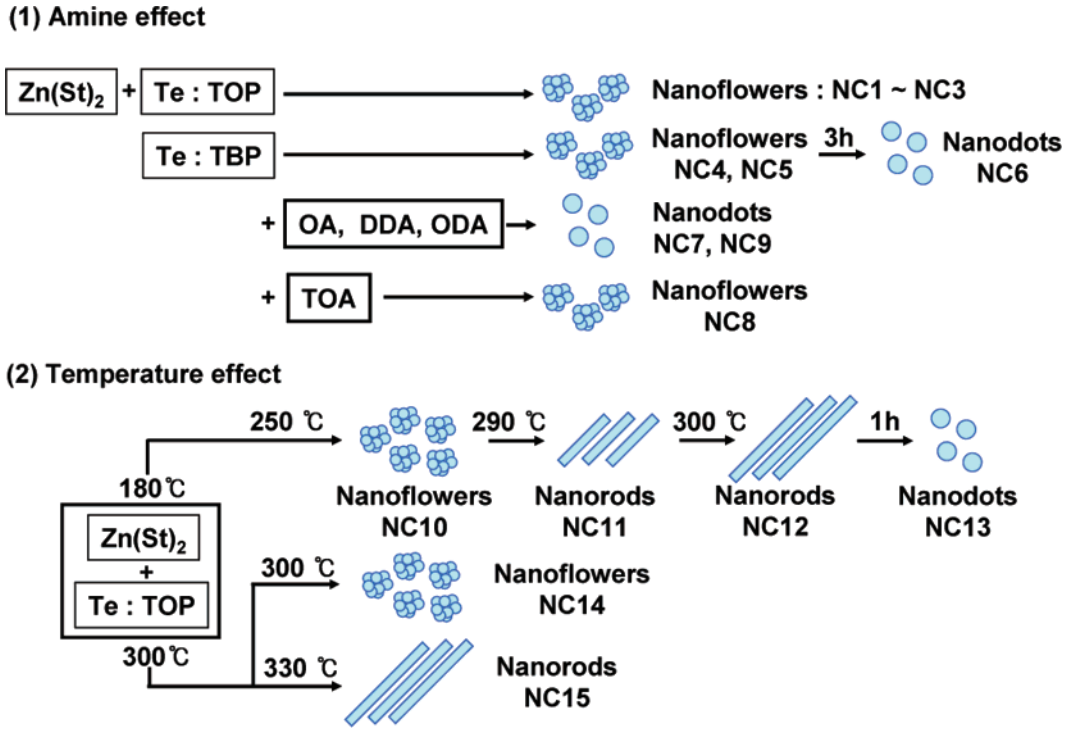

Experimental Procedures

Materials. ODE ($C_{17}H_{34}$═CH_2, tech grade, 90%), Te powders (99.8%), TOP (90%), TBP (97%), OA ($C_8H_{17}-NH_2$, 99%), DDA ($C_{12}H_{25}-NH_2$, 98%), ODA ($C_{18}H_{37}-NH_2$, 90%), and TOA ($(C_8H_{17})_3-N$, 98%) were purchased from Aldrich, and zinc stearate ($Zn(St)_2$, $[CH_3-(CH_2)_{16}COO]_2Zn$, EP grade) was obtained from Junsei. All chemicals were used without further purification.

Synthetic Procedure. *Various Concentrations of TOP and TBP.* The procedure was divided into three steps: (1) $Zn(St)_2$ (0.1 mmol) was mixed with 9.5 mL of ODE in a 25 mL three-necked flask equipped with a condenser, and the mixture was heated to 300 °C under argon flow. (2) A solution of Te (0.2 mmol) in 0.5 mL (1.0 mmol), 1.5 mL (3.0 mmol), or 2.0 mL (4 mmol) of TOP (or TBP) was swiftly injected into the heated solution, and the reaction mixture was then cooled to 270 °C. (3) The mixture was maintained at 270 °C for 10 min to allow for growth of the ZnTe NCs. To monitor the size and shape evolution as a function of growth time, the mixture was incubated at this temperature for 3 h.

Addition of Amines. In step 2, OA, DDA, ODA, or TOA was dissolved in the Te−TOP solution and injected into the hot solution. The other reaction conditions were kept the same as those described previously.

Change of Growth Temperature. The growth temperature was altered as follows: in step 1, the mixture was heated to 180 °C instead 300 °C. In step 2, a Te−TOP solution was injected into the solution at 180 °C. Aliquots were taken from the reaction mixture when the temperature reached 250, 290, and 300 °C to monitor morphology. In step 3, the reaction at 300 °C was stopped after 1 h by removing the heating mantle. Alternatively, the injection temperature of the Te−TOP solution was 300 °C in step 2, but the growth temperature (in step 3) was varied to 300 °C (or 330 °C) and the growth time to 10 min.

After the reaction mixture cooled to approximately 40 °C, purification of the NCs was carried out by repeatedly extracting the unreacted precursors from the reaction mixture dissolved in hexane by adding methanol, and the ZnTe NCs were isolated by precipitation with acetone. The aliquots diluted with hexane were used without further purification to monitor the morphology of the ZnTe NCs.

Characterization. The products were characterized by field-emission transmission electron microscopy (FE TEM, FEI TECNAI G2 200 kV and Jeol JEM 2100F) and high-voltage TEM (HVEM, Jeol JEM ARM 1300S, 1.25 MV). High-resolution X-ray diffraction (XRD) patterns were obtained using the 8C2 beam line of the Pohang Light Source (PLS) with monochromatic radiation (λ = 1.54520 Å) and the Cu Kα line (λ = 1.5406 Å) of a laboratory−based diffractometer (Philips X'Pert PRO MRD). The X-ray photoelectron spectroscopy (XPS) measurements were performed at the U7 beam line of the PLS and using a laboratory−-based spectrometer (XPS, ESCALAB 250, VG Scientifics) with a photon energy of 1486.6 eV (Al Kα). Raman spectroscopy (Renishaw 1000) was measured using the 514.5 nm line of an argon ion laser. UV−vis spectroscopy (Scinco S-3100) was used to identify the growth of the ZnTe NCs. Steady-state photoluminescence (PL) measurements were carried out using an He−Cd laser (λ = 325 nm) as the excitation source. The laser power was below 1 MW/cm^2.

Results and Discussion

The synthetic procedure and various shapes of the labeled products are summarized in Scheme 1. The growth condition and shape and size of the ZnTe NCs synthesized are listed in Table 1.

Synthesis of ZnTe NCs Using Various Concentrations of TOP or TBP. Figure 1a−c displays TEM images of the ZnTe NCs synthesized using Zn/Te/TOP ratios of 1:2:10, 1:2:30, and 1:2:40, respectively. The respective ZnTe NCs (NC1 to ~NC3) all showed unique, 3-D, flower-like nanostructures consisting of a number of aggregated, dot-shaped NCs (nanodots), which are hereafter referred to as nanoflowers. The inset of Figure 1 corresponds to the magnified

Table 1. Growth Condition and Shape and Size of ZnTe NCs Synthesized in This Study

NC	Zn/Te/TOP/amines	amines	injection temp. (°C)	growth temp. (°C)	growth time	shape	av size of NCs (nm)
1	1:2:10:0		300	270	10 min	flowers (18 nm)[a]	4
2	1:2:30:0		300	270	10 min	flowers (23 nm)	4
3	1:2:40:0		300	270	10 min	flowers (50 nm)	5
4	1:2:10:0[b]		300	270	10 min	flowers (20 nm)	6
5	1:2:40:0[b]		300	270	10 min	flowers (120 nm)	7
6	1:2:30:0		300	270	3 h	dots	9
7	1:2:30:10	OA	300	270	10 min	dots	8
8	1:2:30:10	TOA	300	270	10 min	flowers (60 nm)	11
9	1:6:24:5[b]	ODA	300	270	10 min	dots	14
10	1:2:30:0		180	250	~5 min	flowers (20 nm)/rods	35/30 (6)[c]
11	1:2:30:0		180	290	~7 min	rods/flowers	12/160 (13)[c]
12	1:2:30:0		180	300	~9 min	rods/flowers	18/300 (17)[c]
13	1:2:30:0		180	300	~1 h	dots	7
14	1:2:30:0		300	300	10 min	flowers (30 nm)	7
15	1:2:30:0		300	330	10 min	rods	25/450 (18)[c]

[a] In the case of nanoflowers, the size of flowers. [b] TBP used instead of TOP. [c] In the case of nanorods, the diameter/length (aspect ratio).

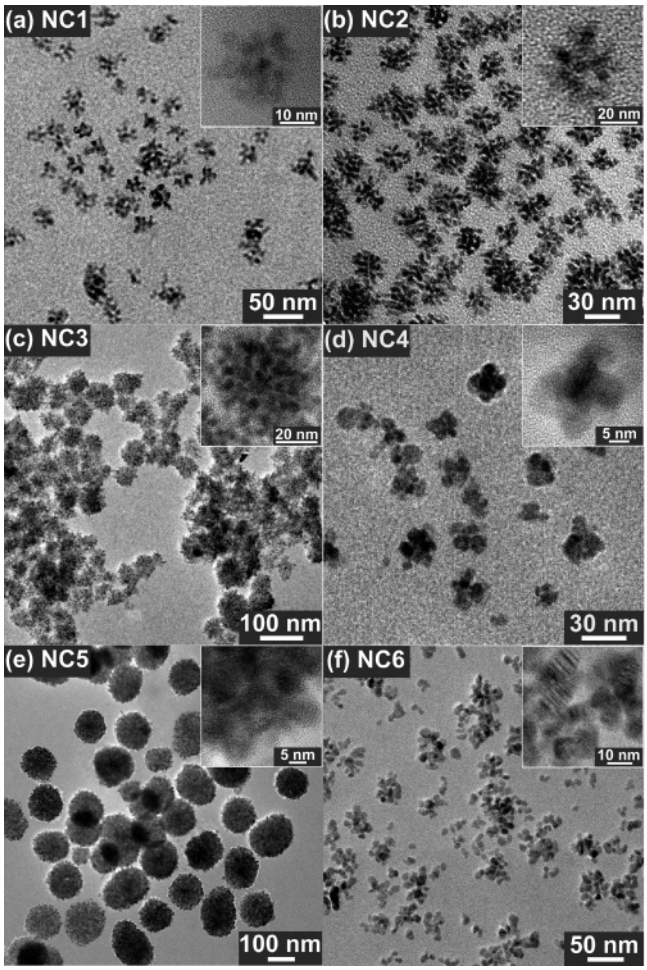

Figure 1. TEM images of ZnTe nanoflowers grown for 10 min at 270 °C using a molar ratio of Zn/TOP of (a) 1:10 (NC1), (b) 1:30 (NC2), and (c) 1:40 (NC3) and using a molar ratio of Zn/TBP of (d) 1:10 (NC4) and (e) 1:40 (NC5). (f) TEM image of dispersed ZnTe nanodots after incubation of NC2 for 3 h (NC6).

image of the individual nanoflower, showing the size of the nanodots. The average size of the nanodots and nanoflowers is 4 ± 0.4 and 18 ± 3 nm for NC1, 4 ± 0.4 and 23 ± 3 nm for NC2, and 5 ± 0.5 and 50 ± 5 nm for NC3. There is not much increase in the size for NC1 and NC2. Nevertheless, as the concentration of TOP increases, the size of both nanodots and nanoflowers shows a tendency of increase.

Nanoflowers were also produced when TBP was used instead of TOP in a solution containing Zn/Te/TBP at a ratio of 1:2:10 and 1:2:40, as shown in Figure 1d,e. The respective ZnTe NCs are denoted as NC4 and NC5. As the concentration of TBP increased, the average size of the nanodots increased from 6 ± 0.6 to 7 ± 0.7 nm (insets in Figure 1d,e), and that of the nanoflowers increased from 20 ± 3 to 120 ± 10 nm. When incubated at the growth temperature, these nanoflowers separated into nanodots. As seen in Figure 1f, the average size of dispersed nanodots (NC6) grown from a mixture of Zn/Te/TOP at a 1:2:30 ratio increased to 9 ± 1 nm (inset of Figure 1f) after 3 h of growth.

Peng and co-workers previously demonstrated the formation of In_2O_3, CoO, MnO, ZnO, and ZnSe nanoflowers using the limited ligand protection strategy, in which freshly formed NCs undergo 3-D aggregation when the amount of ligands is below the critical concentration necessary for stabilization of the individual NCs.[19] Formation of ZnTe nanoflowers in this study can also be explained by the limited ligand protection strategy. Assuming that the limited ligand protection strategy was occurring, excess TOP (or TBP) remaining after Te was activated would serve as a ligand, but its bulky alkyl chains would induce aggregation of the ZnTe nanodots into flower-like nanostructures. The large steric hindrance of the tertiary phosphine chains would reduce the degree of surface protection afforded the ZnTe NCs, which would provide the kinetic driving force needed for the 3-D oriented attachment, and the formation of 3-D aggregates by intermolecular interactions would be thermodynamically allowed because of the reduced surface free energy of the individual NCs.[19] In addition, its 3-D geometrical structure of TOP and TBP appears to be effective at inducing the 3-D oriented attachment of the ZnTe NCs.

The constant formation of the ZnTe nanoflowers over a wide concentration range indicates that TOP (or TBP) remains as the limit protection ligand. The increased size of the dots and flowers as a result of an increased TOP (or TBP) concentration could be explained by the concurrent role of TOP (or TBP) as the activating agent for Te. As the concentration of TOP (or TBP) increases, the increased concentration of the activated Te/TOP may produce higher yield, larger diameter ZnTe NCs, which in turn would cause the ZnTe NCs to be more likely to aggregate and form nanoflowers. TBP has shorter and more compact alkyl chains than TOP, which would permit the growth of the larger

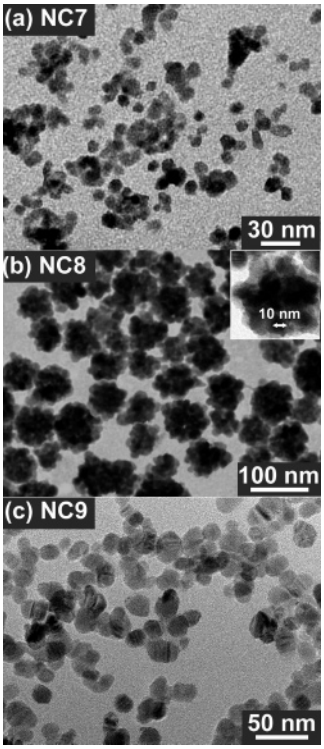

Figure 2. TEM images of ZnTe NCs synthesized using (a) OA (NC7), (b) TOA (NC8), and (c) ODA (NC9).

nanodots, which is consistent with previous studies.[20] The larger nanoflowers would, in turn, be formed by their smaller ligand protection ability to the nanocrystals. For both TOP and TBP, the nanoflowers are separated into individual nanodots by sufficient thermal energy, confirming the thermodynamically unstable nature of the nanoflowers.

Evolution of the Morphology Using Amines. Figure 2a,b displays the TEM images of the ZnTe NCs synthesized with OA and TOA, respectively. The NCs are denoted as NC7 and NC8, respectively. The ratio of Zn/Te/TOP/amine was 1:2:30:10, and the reaction time was 10 min. The amines served as both the activating agent of $Zn(St)_2$ and the surfactants. When the primary amines OA (C8), DDA (C12), and ODA (C18) were added at the same molar ratio, no nanoflowers were produced, but separate nanodots (NC7) with an average size of 8 ± 0.8 nm were consistently produced, irrespective of the alkyl chain length, as shown in Figure 2a. In contrast, when the tertiary amine TOA (C8 $\times$ 3) was added, stable nanoflowers (NC8) were produced (Figure 2b). The inset of Figure 2b corresponds to the magnified image of the individual nanoflower. The average size of the nanoflowers (60 ± 5 nm) and the individual NCs (11 ± 1 nm) was much larger than that of the nanoflowers produced without amines (NC2; flower size = 23 nm and dot size = 4 nm).

The addition of a sufficient amount of OA, DDA, and ODA probably significantly enhanced the degree of ligand protection and stabilized the ZnTe nanodots in a dispersed form. However, when TOA is used, the system remains in the limited ligand protection mode. The larger steric factors of the tertiary alkyl chains of TOA, as compared to those of the primary amines (OA, DDA, and ODA), but probably comparable to that of TOP, may result in insufficient surface coverage to induce the 3-D aggregation of the nanodots. The larger size of the nanodots, as compared to the case of primary amines, results from their larger steric hindrance.

To produce the well-dispersed larger size spherical-shaped nanodots, we used ODA and TBP without altering the growth temperature. Figure 2c shows the efficient production of ZnTe nanodots (av diameter = 14 ± 1 nm), resulting from using a solution of Zn/Te/TBP/ODA in a ratio of 1:6:24:5 (NC9). When TOP was used in place of TBP, the growth of the short tripod- and tetrapod-like NCs became feasible, as is shown in the Supporting Information Figure S1. The average size of these NCs was approximately 8 nm. These results are consistent with the previous observation that TBP yields dot-shaped CdTe NCs, whereas TOP allows the growth of elongated NCs, such as tetrapods.[21]

Temporal Shape Evolution by Growth Temperature. To study shape evolution as a function of growth temperature, the growth temperature was increased at a rate of 13 °C/min, followed by injection of a Te−TOP mixture into the $Zn(St)_2$−ODE solution (using the same concentration as that of NC2) at 180 °C. The reaction mixture turned brown at ~230 °C, indicating that formation of the ZnTe NCs starts at this temperature. Aliquots were taken from the reaction mixture at temperatures of 250, 290, and 300 °C. Figure 3a−c corresponds to the TEM images of the ZnTe NCs, taken at respective temperatures. The shapes of the ZnTe NCs produced at 250 °C (NC10) are exclusively a nanoflower attached to one nanorod (av diameter = 5 ± 0.5 nm, length = 30 ± 5 nm, and aspect ratio = 6). The nanoflowers (av size of 20 ± 5 nm) are comprised of nanodots (av size = 3 ± 0.3 nm), as shown in the inset to Figure 3a. At 290 and 300 °C, the thicker and longer rod-shaped ZnTe NCs appear with the nanoflowers. The average diameter, length, and aspect ratio increase with temperature (av diameter = 12 ± 1 nm, length = 160 ± 10 nm, and aspect ratio = ~13 at 290 °C (NC11) and diameter = 18 ± 2 nm, length = 300 ± 10, and aspect ratio = ~17 at 300 °C (NC12)). The dispersed ZnTe nanodots (av size = 7 ± 0.7 nm; NC13) are produced after incubation of the reaction mixture at 300 °C for 1 h.

On the basis of these TEM images, the temporal shape evolution of the ZnTe NCs can be described as follows. At lower temperatures, thermodynamically stable nanodots are formed due to the low concentration of monomers and then aggregated into nanoflowers following the mechanism described previously. As the temperature increases, the concentration of monomers in the bulk solution becomes higher, followed by elongated growth along the higher surface energy (110) planes, which will be shown in the following HRTEM analysis, to form nanorods.[22] This evolution from nanodots (in an aggregated form of nanoflowers) to nanorods with increasing monomer concentration is consistent with that of other II−VI semiconductors (e.g.,

(20) Murray, C. B.; Sun, S.; Gaschler, W.; Doyle, H.; Betley, T. A.; Kagan, C. R. *IBM J. Res. Dev.* **2001**, *45*, 47.
(21) Yu, W. W.; Wang, Y. A.; Peng, X. *Chem. Mater.* **2003**, *15*, 4300.
(22) Jun, Y.-W.; Choi, J.-S.; Cheon, J. *Angew. Chem., Int. Ed.* **2006**, *45*, 3414.

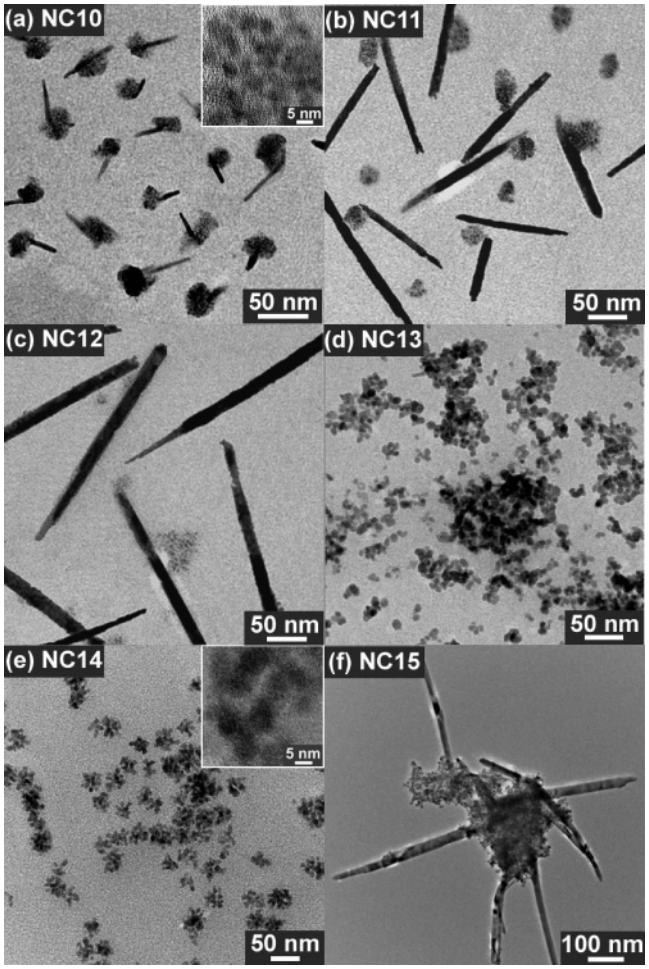

Figure 3. TEM images of ZnTe NCs synthesized when the temperature reached (a) 250 °C (NC10), (b) 290 °C, (NC11), and (c) 300 °C (NC12), after the injection of the Te/TOP mixture at 180 °C, and (d) 300 °C (NC13) for 1 h. TEM images of ZnTe NCs grown when the injection/growth temperatures are (e) 300/300 °C (NC14) and (f) 300/330 °C (NC15), for 10 min.

CdSe) NCs.[23,24] The increased concentration of monomers at higher temperatures would induce an increase of the diameter and length of the nanorods. It is surprising that the ZnTe nanodots are produced after incubation of the reaction mixture. We suggest that the ZnTe nanorods are initially grown by a kinetically controlled growth reaction but that the ZnTe nanodots, which are the most thermodynamically stable form, are eventually formed due to sufficient thermal energy.[23,24]

To verify that the formation of nanorods occurs in the presence of higher concentrations of monomers, the growth temperature was set at 300 and 330 °C for 10 min, using the concentration of NC2 (Zn/Te/TOP = 1:2:30). At 300 °C, nanoflowers (av size = 30 ± 5 nm, NC14) comprised of nanodots with an average size of 7 ± 0.7 nm were formed, which is somewhat larger than those grown at 270 °C (NC2). At 330 °C, both nanorods (diameter 25 ± 3 nm, length 450 ± 30 nm, and aspect ratio = ~18) and nanodots (ca. 7 nm) were observed (NC15). These results are consistent with the results described previously (NC10−NC12), showing that a higher growth temperature (i.e., higher monomer concentration) induces the formation of the elongated shape.

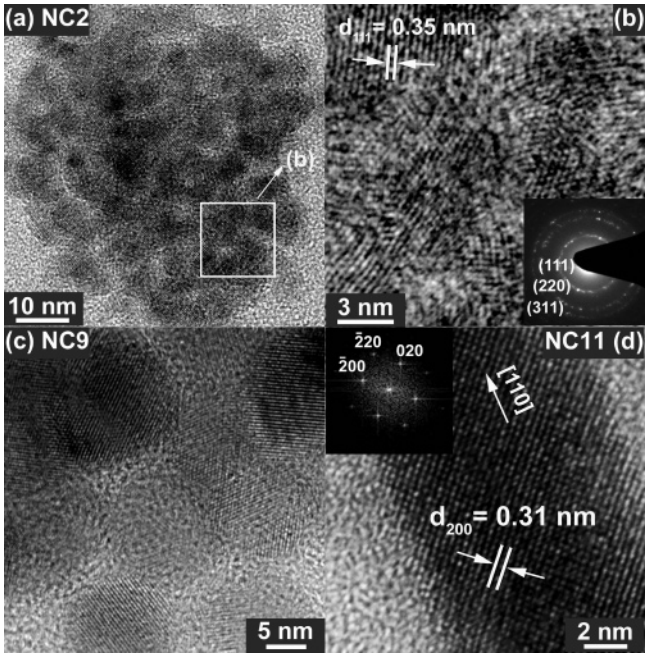

Figure 4. (a) HRTEM image of a nanoflower (NC2) with a size of 30 nm and (b) atomic-resolved image of the single-crystalline ZnTe nanodots (size = 4 nm) and corresponding SAED pattern (inset). (c) HRTEM image of nanodots (NC9) with an av size of 14 nm. (d) HRTEM images of nanorods (NC11), grown along the [110] direction. Inset displays the corresponding FFT ED pattern. Highly crystalline (111) planes are separated by $d = 0.35$ nm.

HRTEM Images and XRD. The EDX analysis confirms that the NCs were comprised of Zn and Te at a ratio of 1 ± 0.1, as shown in the Supporting Information Figure S2. Figure 4a shows the high-resolution TEM (HRTEM) image of a ZnTe nanoflower synthesized without any amines (NC2). The magnified image of a selected area (shown in Figure 4a) and the corresponding selected area electron diffraction (SAED) pattern reveals that the individual nanodots consisted of a single-crystalline cubic unit cell of ZnTe (Figure 4b and inset). The highly crystalline (111) planes are separated by $d = 0.35$ nm (JCPDS no. 15−0746; $a = 6.1026$ Å). The HRTEM image of the nanodots (NC9) with a size of 14 nm is shown in Figure 4c. This image confirms the formation of highly crystalline spherical-shaped ZnTe nanocrystals. Figure 4d and the inset show the HRTEM image and corresponding fast Fourier transform ED (FFT ED) of the nanorods (NC11), respectively. The single-crystalline ZnTe NCs grow along the [110] direction. The (200) plane fringes are separated by about 3.1 nm.

The XRD patterns of the ZnTe powders (Aldrich, 99.99%), nanoflowers (NC2), and nanodots (NC9) are shown in Figure 5. They show peaks corresponding to cubic ZnTe (JCPDS no. 15−0746; $a = 6.1026$ Å). Using the Debye−Scherrer equation, the average sizes of the nanodots were estimated to be 5 and 15 nm for NC2 and NC9, respectively. The ZnTe NCs show a peak (marked by an asterisk) corresponding to the TeO_2 (JCPDS no. 09−0433; orthorhombic, $a = 5.607$ Å, $b = 12.034$ Å, and $c = 5.463$ Å) phase, which probably formed at the surface of the NCs. The powders also contain TeO_2 impurities. The XPS and Raman spectra of the ZnTe

(23) Peng, Z. A.; Peng, X. *J. Am. Chem. Soc.* **2002**, *124*, 3343.
(24) Peng, Z. A.; Peng, X. *J. Am. Chem. Soc.* **2001**, *123*, 1389.

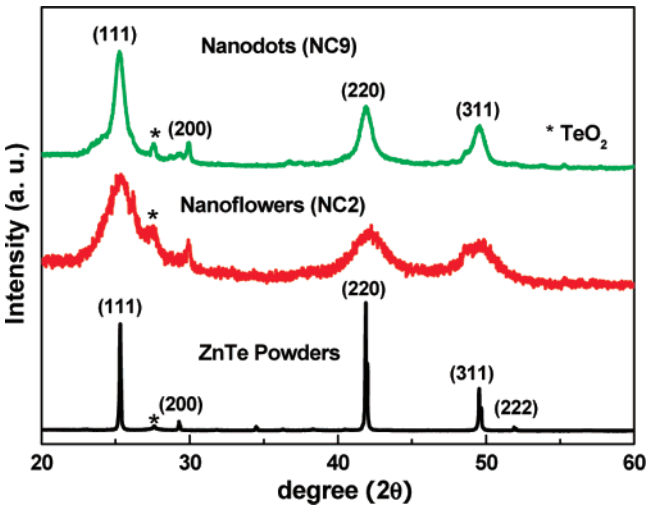

Figure 5. XRD patterns of the ZnTe powders (Aldrich, 99.99%), nanoflowers (NC2), and nanodots (NC9).

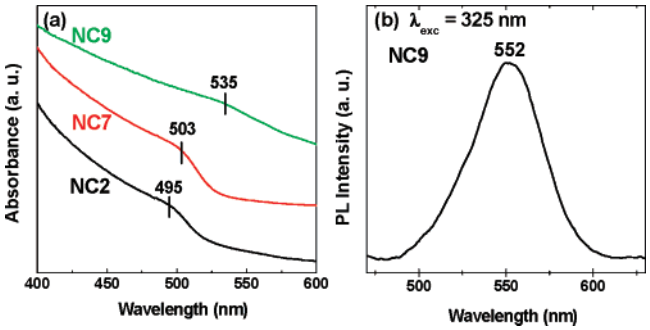

Figure 6. (a) UV−vis absorption spectrum of nanoflowers (NC2, av size of nanodots = 4 nm) and two nanodots: NC7 (av size = 8 nm) and NC9 (av size = 14 nm). (b) PL spectrum of NC9. Excitation wavelength is 325 nm (3.815 eV) from an He−Cd laser.

NCs are shown in Supporting Information Figures S3 and S4, respectively, confirming the presence of pure highly crystalline ZnTe nanocrystals.

Optical Properties. Figure 6a shows the UV−vis absorption of the nanoflowers (NC2, av size of nanodots = 4 nm) and two nanodots: NC7 (av size = 8 nm) and NC9 (av size = 14 nm). As the size of the NCs increases, the absorption band shows a red shift due to the quantum size effect: 495 nm (2.51 eV) for 4 nm, 503 nm (2.47 eV) for 8 nm, and 535 nm (2.32 eV) for 14 nm. Figure 6b shows the PL spectrum of NC9. The excitation wavelength of the PL is 325 nm (3.815 eV) from a He−Cd laser. The peak appears at 552 nm (2.25 eV). On the basis of the band gap derived from the UV−vis absorption, this band would correspond to the near band edge emission. We could not obtain the PL spectrum of NC2 and NC7, due to the intrinsic low quantum yield (ca. <0.01) of ZnTe NCs, and a background signal from the residual ligands in the region of 400−500 nm.

The absorption band of NC2 appears at a lower energy region than that reported by Cheon and co-workers (i.e., 340 nm (PL peak at 380 nm) for 4.2 nm and 430 nm (PL peak at 450 nm) for 5.4 nm ZnTe NCs).[14] Basché and co-workers reported the absorption at 440 nm for 4.5 nm unshelled ZnTe NCs (with no PL data).[15] In contrast to those dispersed nanocrystals, the present nanodots aggregate to form flowers under a limited ligand protection regime, and they are probably under a stronger interaction with other aggregated nanodots, which may induce a lower energy shift of the absorption. Further studies are needed to clarify the position of absorption and PL emission.

Conclusion

We synthesized highly crystalline ZnTe NCs with a controlled shape using various ligands and growth temperatures and times. The reaction of $Zn(St)_2$, TOP (or TBP), and Te at a molar ratio of 1:2:10−40 in ODE solution at 270 °C produced 3-D nanoflowers (av size = 20−120 nm) that consisted of a number of nanodots (av size = 4−7 nm). We used amines such as OA, DDA, ODA, and TOA as the activation agents for $Zn(St)_2$. Dispersed nanodots were produced when OA, DDA, or ODA were used, but nanoflowers (av size = 60 nm) that were comprised of a number of nanodots (av size = 11 nm) were produced with TOA. These results indicate that the steric hindrance of tertiary alkyl chains of TOP, TBP, and TOA would induce aggregation of nanodots, forming nanoflowers. These thermodynamically unstable nanoflowers are dispersed into nanodots after incubation of the reaction mixture. Moreover, the temporal shape evolution from nanodots (in the form of nanoflowers) to nanorods was monitored by increasing the growth temperature. These nanorods eventually evolved into nanodots after incubation. We suggest that the ZnTe nanorods were produced under a kinetically controlled growth condition and evolved to thermodynamically stable nanodots.

Acknowledgment. This work was supported by KRF grants (R14-2003-033-01003-0, R02-2004-000-10025-0, and 2003-015 C00265) and BK21. The SEM, HVEM, XRD, and XPS measurements were performed at the Korea Basic Science Institute. The experiments at the PLS were partially supported by MOST and POSTECH.

Supporting Information Available: Additional TEM image, EDX, XPS, and Raman spectrum of ZnTe NCs. This material is available free of charge via the Internet at http://pubs.acs.org.

CM0711360